Research Paper

lncRNA MEG3 aggravated neuropathic pain and astrocyte overaction through mediating miR-130a-5p/CXCL12/CXCR4 axis

Jiacai Dong[1], Rui Xia[2], Zhonggui Zhang[3], Cheng Xu[3]

[1]Department of Anesthesiology, Qianjiang Hospital Affiliated to Renmin Hospital of Wuhan University, Qianjiang 433100, Hubei, China
[2]Department of Anesthesiology, The First People's Hospital of Jingzhou, Jingzhou 434000, Hubei, China
[3]Department of Pain, The First People's Hospital of Jingzhou, Jingzhou 434000, Hubei, China

Correspondence to: Cheng Xu; **email:** xun329552828548414@163.com, https://orcid.org/0000-0001-5324-9481
Keywords: MEG3, miR-130a-5p, neuropathic pain, CXCL12, astrocytes
Received: June 15, 2021 **Accepted:** September 20, 2021 **Published:** October 5, 2021

Copyright: © 2021 Dong et al. This is an open access article distributed under the terms of the Creative Commons Attribution License (CC BY 3.0), which permits unrestricted use, distribution, and reproduction in any medium, provided the original author and source are credited.

ABSTRACT

Objective: Long non-coding RNAs (lncRNAs) exert a critical function in mediating neuropathic pain (NP). MEG3, a novel lncRNA, contributes to astrocyte activation and inflammation. However, its role in NP remains unclear.
Methods: The chronic constriction injury (CCI) method was employed to construct an NP rat model. Astrocyte activation was induced by lipopolysaccharide (LPS). The profiles of MEG3, microRNA (miR)-130a-5p, CXC motif chemokine receptor 12 (CXCL12)/CXC motif chemokine receptor 4 (CXCR4), and the Rac1/NF-κB pathway in CCI rats' spinal cord tissues and astrocytes were monitored by reverse transcription-quantitative PCR (RT-qPCR) and western blot (WB). Pain scores of CCI rats were assessed. Enzyme-linked immunosorbent assay (ELISA) was adopted to monitor neuroinflammation alteration. The glial fibrillary acidic protein (GFAP)-labeled astrocytes were tested by immunohistochemistry (IHC). Bioinformatics, dual-luciferase reporter assay and RNA immunoprecipitation (RIP) were utilized to verify the molecular mechanism between MEG3 and miR-130a-3p.
Results: MEG3, CXCL12 and CXCR4 were overexpressed and miR-130a-5p was knocked down in CCI rats and LPS-induced astrocytes. Up-regulating MEG3 aggravated NP, enhanced inflammatory cytokines interleukin-1β (IL-1β), tumor necrosis factor (TNF)-α, and interleukin-6 (IL-6) expression and release in CCI rats and LPS-induced astrocytes. Up-regulating miR-130-5p repressed LPS-induced inflammation in astrocytes. AS verified by the dual-luciferase reporter assay and RIP assay, MEG3 sponged miR-130a-5p as a competitive endogenous RNA (ceRNA). What's more, miR-130a-5p up-regulation weakened the MEG3-induced proinflammatory effects on LPS-induced astrocytes.
Conclusions: MEG3 aggravates NP and astrocyte activation via the miR-130a-5p/CXCL12/CXCR4 axis, which is a potential therapeutic target for NP.

INTRODUCTION

Neuropathic pain (NP) is a chronic secondary pain resulting from illness or injury to the nervous system, affecting up to 8% of the population [1]. NP is commonly caused by diabetes, reactivation of herpes zoster, nerve compression or radiculopathy, alcohol consumption, chemotherapy or certain drug abuse, and trigeminal neuralgia [2]. It is characterized by an abnormal hypersensitivity to stimuli (hyperalgesia) and a nociceptive response to non-harmful stimuli (abnormal pain) [3]. Neuroinflammation is closely related to NP, and inflammation-induced microglial activation and astrocytes contribute to NP evolvement [4]. Current recommended first-line therapies include antidepressants (tricyclic agents and serotonin-norepinephrine reuptake inhibitors) and anticonvulsants (gabapentin and pregabalin) [5]. However, in some

cases, medication alone cannot control chronic pain. Therefore, it is of great significance to find new treatments for NP.

Long non-coding RNAs (lncRNAs) are small RNAs, which are reported to be closely linked to NP [6]. For example, lncRNA SNHG1 is up-regulated in rats undergoing spinal nerve ligation (SNL), and inhibiting SNHG1 alleviates NP [7]. LncRNA GAS5 is down-regulated in chronic constriction injury (CCI) rats, and GAS5 overexpression represses the expression of inflammatory factors in spinal cord tissues and alleviates NP [8]. Also, lncRNA MRAK009713 [9], KCNA2-AS [10], LncRNA H19 [11], etc., participate in the evolvement of NP. As a lncRNA, maternal expression gene 3 (MEG3) functions a role in mediating inflammation [12]. On the one hand, up-regulating MEG3 hampers inflammatory factor production and improves several diseases, such as rheumatoid arthritis [13], ankylosing spondylitis [14] and osteoarthritis [15]. In parallel, MEG3 increases the expression of inflammatory factors in some diseases, including neurological diseases. For instance, enhanced MEG3 level was detectable in mice subjected to cerebral ischemia-reperfusion (I/R) injury and BV2 cells under oxygen-glucose deprivation (OGD)/R treatment. Forced MEG3 overexpression promotes "M1" microglia polarization and inflammatory factor release [16]. In the neonatal mice suffered from hypoxic-ischemic brain damage (HIBD, MEG3 gained a boosted level. MEG3 knockdown declined the neuronal apoptosis rate and the degree of brain atrophy in HIBD mice, enhanced the learning and memory of neonatal HIBD mice [17]. Similarly, MEG3 is up-regulated in the brain tissue of intracerebral hemorrhage (ICH) rats. Abating MEG3 expression restrains edema, neuronal apoptosis, and the release of inflammatory cytokines and oxidative stress in the brain tissue of ICH rats [18]. Therefore, MEG3 can play a role in neuroinflammation.

C-X-C motif chemokine ligand 12 (CXCL12), also known as stromal cell-derived factor-1 (SDF-1), is a CXC chemokine subfamily member and is widely expressed in diversified tissues and cells. CXCL12 specifically interacts with ligands for the G-protein coupled receptors, including CXC motif chemokine receptor 4 (CXCR4) and CXCR7 [19]. Previous studies have exhibited that the CXCL12/CXCR4 signal is involved in modulating NP. For example, in the SNL-induced rat NP model, CXCL12 and CXCR4 are up-regulated in astrocytes and spinal dorsal horn neurons. Inhibiting CXCL12 relieves NP of the SNL rat model [20]. Huang w et al. found that CXCR4 was up-regulated in L4/5 dorsal root ganglion (DRG) in HIV gp120 protein-mediated NP, and inhibiting CXCR4 expression impeded NP [21]. The above studies conclude that the CXCL12/CXCR4 expression is heightened in the NP model, and intervention of CXCL12/CXCR4 may be an effective method in treating NP.

It is well known that lncRNAs sponge miRNAs, thus declining miRNAs' regulatory effects on mRNAs. As the report goes, MEG3 suppresses inflammatory progression by regulating miRNA expression [22]. Additionally, miR-130a-5p is closely related to the inflammatory response [23], and MEG8 reduces the neurological impairment of middle cerebral artery occlusion (MCAO) rats by targeting miR-130a-5p [24]. However, the relationship between MEG3 and miR-130a-5p remains elusive. On the other hand, our study revealed that miR-130a-5p relieves NP following SCI via targeting CXCL12 [25]. Hence, we suppose that MEG3 modulates the CXCL12 expression by targeting miR-130a-5p to dampen CCI-induced NP and neuroinflammation.

MATERIALS AND METHODS

Animals

Forty adult SD rats (female, four-week-old, 180-200 g) were purchased from Wuhan Animal Experimental Center and randomized into the sham and CCI groups. Rats were raised in standard plastic cages at 24±1° C and humidity of 50-70%, with 12-hour light and dark cycles. They could drink and eat freely. The behavioral experiments were conducted between 10 a.m. and 3 p.m., following the National Institutes of Health Guidelines for the Care and Use of Laboratory Animals to alleviate the rats' discomfort or stress. All animal tests were authorized by the Animal Research Committee of Jingzhou First People's Hospital.

The NP rat model

As previously stated [26], the rats were anesthetized with pentobarbital sodium (40 mg/kg), and bilateral sciatic nerve CCI was performed under aseptic conditions. A median thigh incision was made to expose the bilateral sciatic nerve. In contrast, the sciatic nerves in the sham group were exposed and isolated but not ligated. L4 to L6 dorsal spinal cord tissues were harvested on days 0, 1, 3, 5, 7 and 14, respectively.

Construction of lentiviruses

LV-NC (Catalog No. D03003) and the lentiviral vector of LV-MEG3 were synthesized by Shanghai GenePharma Co., Ltd. (Shanghai, China). These lentiviral vectors (1×10^7/0.05 mL) were then injected

into the rats' tail vein three days before the modeling using a micro-needle [27].

Pain thresholds assessment

Mechanical pain was evaluated by Von Frey filaments by adopting a paw withdrawal threshold (PWT) [28]. Briefly, rats were put in a clear plastic box with a metal mesh floor. On days 0, 1, 3, 5, 7, and 14 after CCI, calibrated Von Frey filaments (IITC, Woodland Hills, CA, United States) were employed to generate pressure on the plantar surface of the rat's hind paws. Then, the filament size during claw retraction was monitored. The paw withdraw latency (PWL) was adopted to evaluate hyperalgesia on 0, 1, 3, 5, 7, and 14 days after CCI using a foot-pressure measurement instrument. The hind paws were recorded alternately at 5-minute intervals. The duration between stimulation and paw withdrawal was recorded, and the cutoff time was 30 s.

Immunohistochemistry (IHC)

On the 7th day after the establishment of the CCI rat model, five rats were randomly chosen from each group and executed under chloral hydrate anesthesia. L4 to L6 dorsal spinal cord tissues were collected and stored in 100g/L paraformaldehyde solution and immobilized at room temperature (RT) for 24 hours. Coronal sections (3~4 μM thick) of tissues were placed in an oven for 4~6 hours. Then, the sections were cleaned with PBS three times (2 min each time) and maintained with the rabbit anti-GFAP antibody (Abcam, ab7260, 1: 500, MA, USA) in a refrigerator overnight at 4° C. After washes, the horseradish peroxidase-labeled goat anti-rabbit IgG (1:800) was added and incubated at 37° C for two hours. Afterward, the sections were cleaned, and DAB was adopted for color development. The percentage of area occupied by GFAP-positive astrocytes in the L4 to L6 dorsal spinal cord tissue was assessed with the Image-Pro Plus image analysis software system (Media Cybernetics, MD, USA).

TdT-mediated dUTP nick end labeling (TUNEL) staining

Paraffin sections were processed following the TUNEL Apoptosis Detection Kit instructions. Three sections were taken from each specimen, and five non-overlapping high magnification views of the L4 to L6 dorsal spinal cord tissue were randomly chosen for each section. The TUNEL-positive cell number, i.e., apoptotic cell number, and the total cell number were counted by adopting the Image-Pro Plus image analysis software. The apoptosis index (AI)=apoptotic cell number/total cell number×100%.

Cell culture

Normal human astrocytes (NHAs, isolated from the spinal cord) were commercially provided by American Type Culture Collection (ATCC, Rockville, MD, USA) and grown in the astrocyte medium containing 10% fetal bovine serum (FBS, HyClone, Logan, UT, USA) (AM, Cat. #1801, ScienCell). The medium was altered every 2~3 days, and the cells were sub-cultured every 4~5 days.

Cell transfection

Cells in the logarithmic growth phase were seeded into 6-well plates (5×10^6cells/well) after trypsinization and sub-culture. Cell transfection was carried out after stable cell growth. The pcDNA empty vector (NC), pcDNA-MEG3 (MEG3), miR-130a-5p mimics and the corresponding counterpart fragments were transfected into astrocytes as per the FuGENE®HD Transfection Reagent (Roche, Shanghai, China) guidelines. Cells were maintained at 37° C with 5% CO_2. After transfection for 24 hours, cells were exposed to 100 ng/mL LPS for six hours to 14 days. The control group was left untreated.

Real-time quantitative polymerase chain reaction (qRT-PCR)

MEG3 and miR-130a-5p levels were determined by qRT-PCR. Total RNA was separated using the TRIzol reagent (Invitrogen, CA, USA) and reversely transcribed into first-strand complementary DNA (cDNA) by utilizing the reverse transcription kit (Thermo Fisher Scientific, MA, USA). The miRNA first-strand cDNA synthesis package (Sangon Biotech, Shanghai, China) was adopted for the reverse transcription for miR-130a-3p. The SYBR-Green PCR Master Mix Kit (Applied Biosystems, CA, USA) was employed to amplify the target genes, and the aqMan miRNA analysis kit (Applied Biosystems) was adopted to amplify miR-130a-5p. All amplifications were performed on the 7900HT Fast Real-Time System (Applied Biological System). GAPDH served as the housekeeping gene of MEG3, and U6 served as that of miR-130a-3p. The $2^{-\Delta\Delta\text{-Ct}}$ method was applied for relative expression analysis. Primer sequences of miR-130a-5p were as follows: forward 5'-AACACGC GCTGACTCCTAGT-3', reverse 5'-CAGTGCAGGGT CCGAGGT-3'. MEG3: forward 5'-GTGAAGGTCGG AGTGAACG-3', reverse 5'- CTCGCTCCTGGAAGA TGGTG-3'. GAPDH: forward 5'-CGCTGAGTACGT CGTGGAGTC-3', reverse 5'- GCTGATGATCTTGAG GCTGTTGTC-3'; U6 forward: 5'-GACAGATTCGG TCTGTGGCAC-3', reverse: 5'-GATTACCCGTCGG CCATCGATC-3'.

Western blot (WB)

After tissue and cell treatment, RIPA lysis buffer (Beyotime Biotechnology, Shanghai, China) was added, and the total protein was isolated. Then, 50 g of total protein was subjected to 12% polyacrylamide gel and electrophoresed at 100 V for two hours. It was then electrically transferred to polyvinylidene fluoride (PVDF) membranes (Millipore, MA, USA). After the membranes were sealed with 5% skimmed milk powder at RT for one hour, they were rinsed with TBST three times (10 min each time) and incubated with primary antibodies (1: 1000, Abcam, MA, USA) of iNOS (ab178945), TLR4 (ab13867), COX2 (ab179800), NF-κB (ab32536), p-NF-κB (ab76302), CXCL12 (ab155090), CXCR4 (ab181020), Rac1 (ab155938), and GAPDH (ab9485) overnight at 4° C. After being rinsed in TBST, the membranes were maintained with the horseradish peroxidase (HRP)-labeled anti-rabbit secondary antibody (concentration 1:3000) for one hour at RT. Subsequently, the membranes were subjected to three washes with TBST (10 min each). At last, WB reagents (Invitrogen) were utilized for color development and imaging, and each protein's gray intensity was determined by Image J.

Enzyme-linked immunosorbent assay (ELISA)

L4~L6 dorsal spinal cord tissues were weighed, homogenized by lysate containing protease inhibitors, and centrifuged at 14,000 rpm for 25 min at 4° C to harvest the supernatant. The astrocyte supernatant was collected, centrifuged to remove cell debris, and stored in aliquots at -80° C until being assayed. The interleukin-1β (IL-1β), interleukin-6 (IL-6) and tumor necrosis factor-α (TNF-α) contents in spinal cord tissues and astrocytes were determined by IL-1β, IL-6 and TNF-α ELISA kits (Invitrogen), respectively.

Data analysis

All experiments were repeated three times. The SPSS17.0 statistical software was employed for statistical analysis of the results. Measurement data were presented as "mean ± standard deviation" (x±s). Student t-test was employed to compare the data between two groups. The one-way analysis of variance (ANOVA) was applied to compare the data among multiple groups, followed by the Tukey post hoc test. $P< 0.05$ indicated statistical significance.

Ethics statement

Our study was approved by the Animal Research Committee of Jingzhou First People's Hospital.

Data availability statement

The data sets used and analyzed during the current study are available from the corresponding author on reasonable request.

RESULTS

MEG3 was up-regulated and miR-130a-5p was down-regulated in CCI rat models

To probe the function of MEG3 and miR-130a-5p in NP, we gauged the expression of MEG3, miR-130a-5p and CXCL12/CXCR4 and its downstream Rac1 and NF-κB in L4-L6 dorsal spinal cord tissues of CCI rats and astrocytes following CCI (0, 1, 3, 5, 7, and 14 days) and LPS induction (6 hours, 12 hours, 1 day, 3 days, 7 days, 14 days), using RT-qPCR and WB. As a result, by contrast with the sham group, the MEG3 expression in CCI rats and astrocytes significantly increased (Figure 1A, 1B; $P<0.05$), the miR-130a-5p expression decreased (Figure 1C, 1D; $P <0.05$), the profiles of CXCL12, CXCR4 and Rac1 were elevated, and the NF-κB phosphorylation was facilitated time-dependently (Figure 1E, 1F; $P<0.05$). These findings demonstrated that MEG3, miR-130a-5p and the CXCL12/CXCR4 pathways were involved in NP.

Up-regulating MEG3 promoted NP and inflammation

We injected recombinant lentivirus LV-MEG3 and LV-NC intrathecally into CCI rats to further probe the function of MEG3 in CCI rats. The MEG3 level was examined by RT-qPCR, which disclosed that the MEG3 expression was elevated after transfection with LV-MEG3 (vs. the CCI+LV-NC group) (Figure 2A; $P<0.05$). The rats' NP in each group was assessed using PWT and PWL. The outcomes illustrated that the PWT and PWL of CCI rats were declined with time (vs. the sham group). Transfection with LV-MEG3 further boosted mechanical hypersensitivity and thermal hyperalgesia, as evidenced by a significant decrease in PWT and PWL over time (Figure 2B, 2C; $P< 0.05$). Besides, we examined the number of GFAP-responsive astrocytes in the L4-L6 dorsal spinal cord tissue of CCI rats with IHC. It turned out that the proportion of GFAP-responsive astrocytes was heightened in CCI rats, and it was further elevated after transfection with LV-MEG3 (Figure 2D; $P<0.05$). TUNEL was implemented to verify neuronal apoptosis in the L4-L6 dorsal spinal cord tissue of CCI rats, and the results exhibited that the TUNEL-positive cell number was elevated (vs. the sham group) and was further facilitated after the transfection of LV-MEG3 (Figure 2E; $P<0.05$). To figure out whether MEG3 contributed to inflammation in CCI model rats, we tested the expression

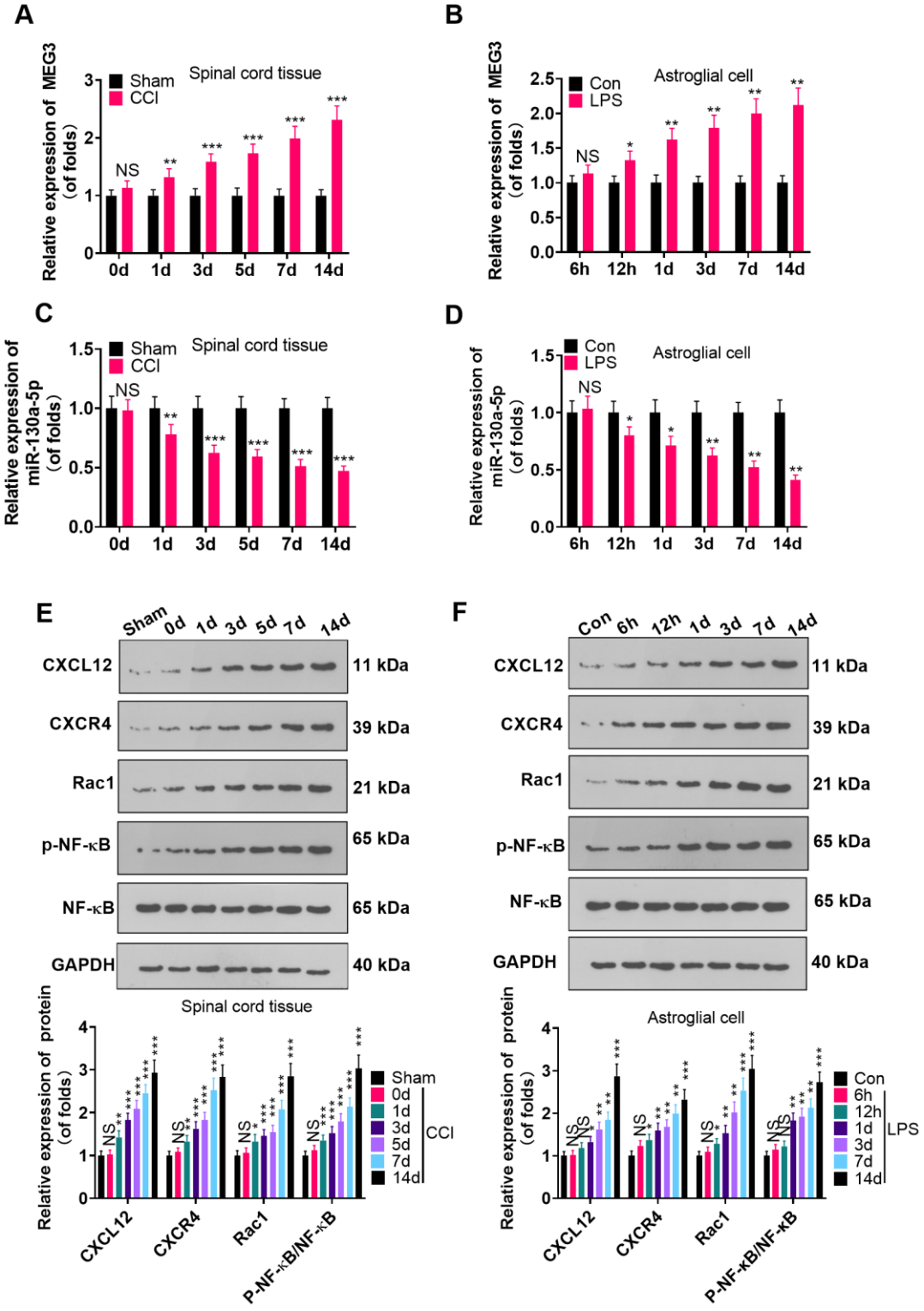

Figure 1. MEG3 was overexpressed and miR-130a-5p was knocked down in CCI rats. (**A**, **B**) The expression of MEG3 in the L4-L6 dorsal spinal cord of CCI rats and astrocytes was assayed by RT-qPCR 0, 1, 3, 5, 7, and 14 days after CCI and 6 hours, 12 hours, 1 day, 3 days, 7 days, and 14 days after LPS induction of astrocytes, respectively. (**C**, **D**) Expression of miR-130a-5p in CCI rats and astrocytes was measured by RT-qPCR at 0, 1, 3, 5, 7, and 14 days after CCI and 6 hours, 12 hours, 1 day, 3 days, 7 days, and 14 days after LPS induction of astrocytes, respectively. (**E**, **F**) Expression of CXCL12/CXCR4 and its downstream Rac1 and NF-κB in the dorsal spinal cord of CCI rats and astrocytes at 0, 1, 3, 5, 7, and 14 days and LPS-induced astrocytes at 6 hours, 12 hours, 1 day, 3 days, 7 days, and 14 days, respectively, was measured using WB. Data were expressed as mean±SD. n=5. NSP>0.05, *P<0.05, **P<0.01, ***P<0.001 (vs. sham group).

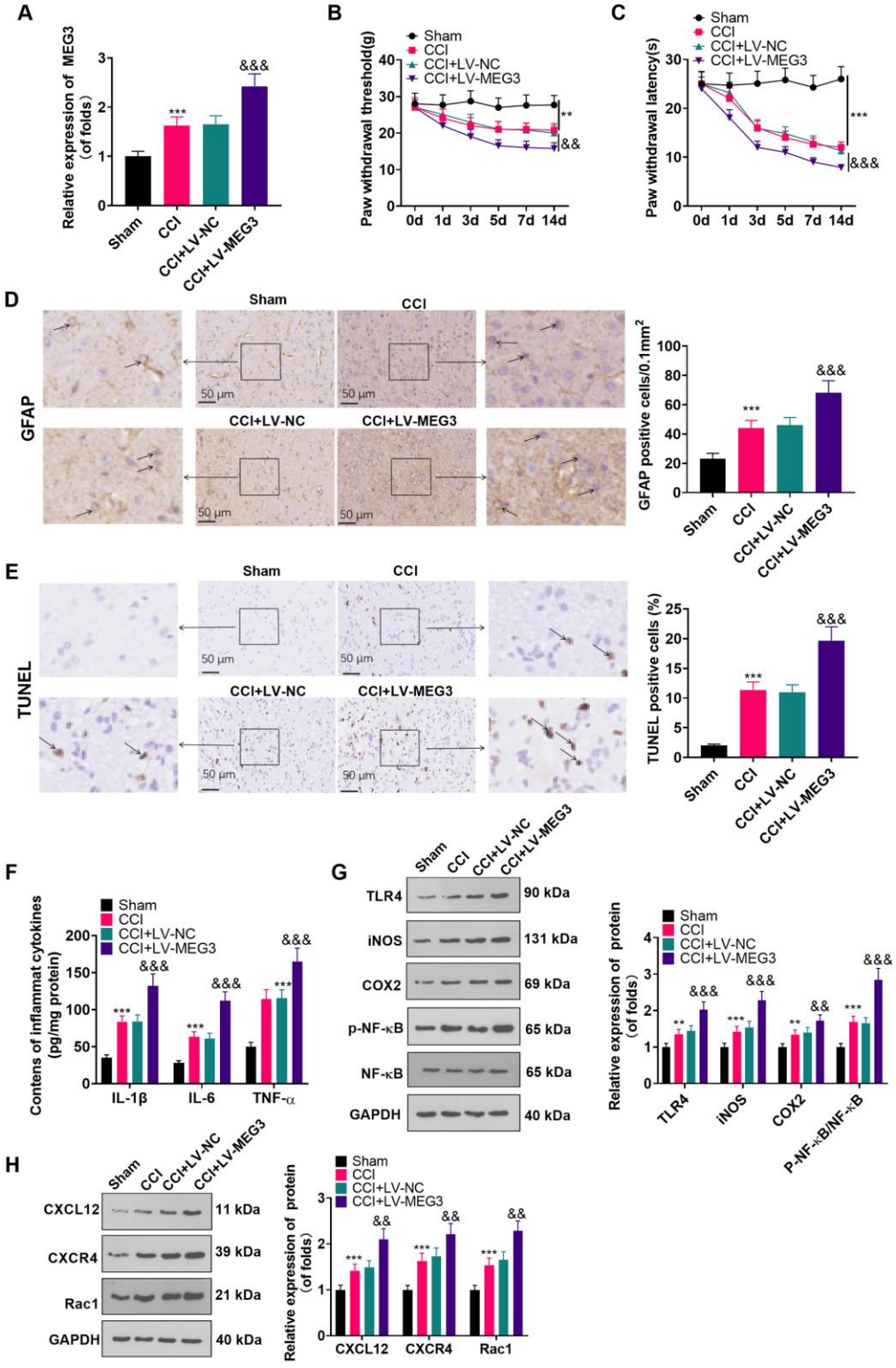

Figure 2. Up-regulation of MEG3 promoted NP and inflammatory response. (**A**) After LV-MEG3 transfection, the level of MEG3 in CCI rats was examined by RT-qPCR. (**B**) PWT was adopted to assess the impact of MEG3 on mechanical hyperalgesia. (**C**) PWL was utilized to evaluate the influence of MEG3 on thermal hyperalgesia. (**D**) The proportion of GFAP-positive cells in CCI rats was determined by IHC; Scale bar=50 μm. (**E**) TUNEL staining was applied to detect the influence of MEG3 on neuronal cell apoptosis in the L4-L6 dorsal spinal cord of CCI rats; Scale bar=50 μm. (**F**) Levels of TNF-α, IL-6 and IL-1β in CCI rats after up-regulating MEG3 were examined by ELISA. (**G**, **H**) The contents of TLR4, COX2, iNOS, NF-κB, CXCL12, CXCR4, and Rac1 in dorsal spinal cord tissues of CCI rats after up-regulating MEG3 were monitored by WB. Data were expressed as mean±SD. n=5. ***P<0.001 (vs. Sham group). &*P*<0.05, &&*P*<0.01, &&&*P*<0.001 (vs. CCI+LV-NC group).

of inflammatory cytokines and inflammatory proteins in the L4-L6 dorsal spinal cord tissues of CCI rats using ELISA and WB. As a result, by contrast with the sham group, the levels of IL-1β, TNF-α and IL-6 were heightened (Figure 2F; $P < 0.05$), the profiles of TLR4, iNOS, COX2, CXCL12, CXCR4, and Rac1 were elevated, and the NF-κB phosphorylation was increased (Figure 2G, 2H; $P< 0.05$) in the CCI group. What's more, these inflammatory factors and inflammatory proteins were further augmented in the MEG3 up-regulation model (Figure 2G, 2H; $P< 0.05$ vs. CCI+Lv-NC group). These data indicated that the up-regulation of MEG3 intensified NP and boosted the levels of inflammatory cytokines in CCI rats.

Up-regulating MEG3 heightened the inflammation of LPS-induced astrocytes

To make certain the function of MEG3 in cells, we transfected MEG3 overexpression plasmids and control vectors (NC-vector) into LPS-induced astrocytes. RT-qPCR demonstrated that MEG3 was up-regulated after transfection with the MEG3 overexpression plasmids compared to that of the LPS+Vector group (Figure 3A; $P<0.05$). The expressions of inflammatory cytokines and inflammatory proteins in LPS-induced astrocytes was determined by ELISA and WB. The results uncovered that inflammatory factors (including IL-1β, TNF-α and IL-6) (Figure 3B–3D; $P<0.05$), as well as inflammatory proteins (including TLR4, iNOS, COX2, p-NF-κB, CXCL12, CXCR4, and Rac1) (Figure 3E–3K; $P<0.05$) were up-regulated in the LPS group (vs. the control group). Additionally, after transfection of MEG3 overexpression plasmids, these inflammatory factors and inflammatory proteins were further increased (Figure 3B–3K; $P<0.05$ vs.LPS+Vector group). Thus, up-regulating MEG3 increased the levels of inflammatory cytokines at the cellular level in astrocyte.

Overexpressing miR-130a-5p impeded LPS-induced astrocyte inflammation

To clarify the role of miR-130a-5p in astrocytes, we transfected miR-130a-3p mimics and controls into LPS-induced astrocytes and checked the miR-130a-3p profile by RT-qPCR. The results illustrated that miR-130a-3p expression was heightened after miR-130a-3p mimics' transfection compared with the LPS+miR-NC group, demonstrating successful transfection (Figure 4A; $P < 0.05$). Then, the biological role of miR-130a-5p in NP was examined by assessing the expression of IL-6, IL-1β and TNF-α. As displayed in Figure 4B–4D, up-regulating miR-130a-3p attenuated the levels of IL-6, IL-1β and TNF-α in astrocytes. Additionally, up-regulating miR-130a-3p distinctly hampered the levels of TLR4, iNOS, COX2, NF-κB phosphorylation, CXCL12, CXCR4, and Rac1 in astrocytes (Figure 4E–4K; $P<0.05$ vs.LPS+miR-NC group). These outcomes corroborated that overexpressing miR-130a-5p hampered inflammation in LPS-induced astrocytes.

MEG3 targeted miR-130a-5p

To investigate the molecular mechanism of MEG3's promoting NP in CCI rats, we predicted miRNAs through the ENCORI (http://starbase.sysu.edu.cn/) database and identified miR-130a-5p as a possible target of MEG3 (Figure 5A). The sequences of wt-MEG3 and mut-MEG3 were constructed into the luciferase reporter vectors. As exhibited, the fluorophore activity was declined in cells cotransfected with miR-130a-5p mimics and wt-MEG3, whereas no obvious effect was observed in the mut-MEG3 group. RIP revealed that miR-130a-5p and MEG3 were dramatically enriched by anti-Ago2 but not anti-IgG in astrocytes (Figure 5C; $P< 0.05$). To ascertain the relationship between miR-130a-5p and MEG3 in astrocytes, we examined the expression of miR-130a-5p as well as CXCL12/CXCR4 and its downstream Rac1 and NF-κB in astrocytes by RT-qPCR and WB after transfection with MEG3 overexpression plasmids or sh-MEG3. As a result, up-regulating MEG3 restrained the miR-130a-5p expression in astrocytes, while down-regulating MEG3 exerted the opposite effects (Figure 5D; $P< 0.05$). Meanwhile, MEG3 overexpression was positively related to the higher expression of CXCL12/CXCR4 and its downstream Rac1, and NF-κB phosphorylation. Contrarily, MEG3 knockdown attenuated CXCL12, CXCR4, Rac1, and NF-κB phosphorylation (Figure 5E; $P<0.05$ vs. sh-NC group). The above results confirmed that MEG3 targeted and inhibited miR-130a-5p.

Overexpressing miR-130a-5p reversed the inflammatory response in MEG3-mediated astrocytes

The connection between miR-130a-5p and MEG3 in cells had been verified previously. To clarify whether MEG3 interacted with CXCL12 through miR-130a-5p, we added miR-130a-5p mimics in LPS-induced astrocytes and gauged the expression of MEG3, miR-130a-5p and CXCL12/CXCR4 and its downstream factors Rac1 and NF-κB by RT-qPCR and WB. As expected, compared with the LPS+MEG3 group, transfection of miR-130a-5p mimics resulted in up-regulation of miR-130a-5p and down-regulation of MEG3, CXCR4, and Rac1 (Figure 6A–6C; $P<0.05$). Besides, in comparison to the LPS+MEG3 group, the levels of inflammatory factors (Figure 6D–6F; $P<0.05$) and inflammatory proteins, including TLR4, iNOS,

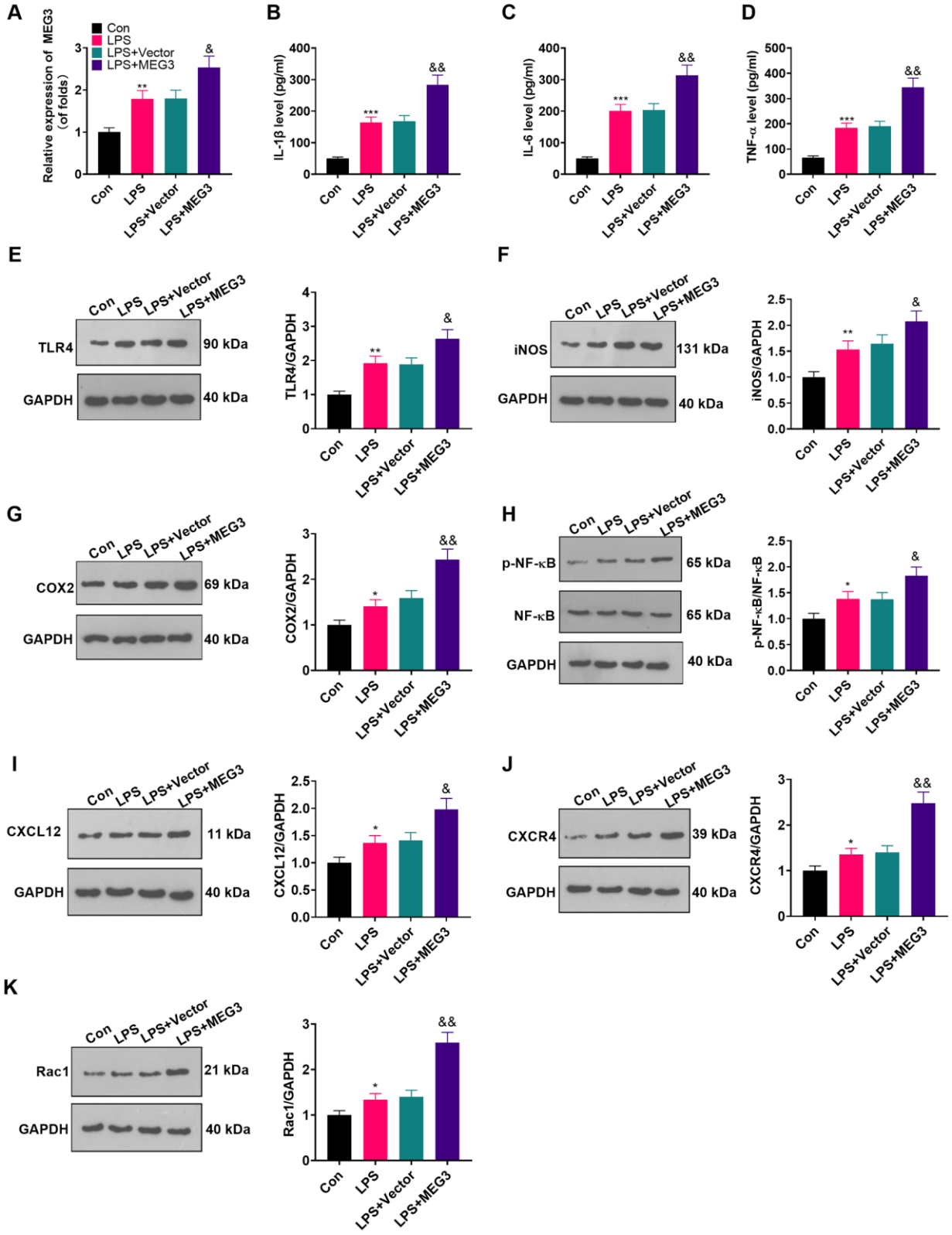

Figure 3. Up-regulating MEG3 facilitated LPS-induced astrocyte inflammation. (**A**) After transfection of MEG3 overexpressing plasmids, the level of MEG3 in astrocytes was tested by RT-qPCR. (**B**–**D**) The contents of IL-1β (**B**), IL-6 (**C**), TNF-α (**D**) in astrocytes were monitored by ELISA after MEG3 up-regulation. (**E**–**H**) The levels of TLR4 (**E**), iNOS (**F**), COX2 (**G**), NF-κB (**H**), CXCL12 (**I**), CXCR4 (**J**), and Rac1 (**K**) in astrocytes after up-regulation of MEG3 were compared by WB. Data were expressed as mean±SD. n=3. ***P*<0.01, ****P*<0.001 (vs. LPS group). &*P*<0.05, &&*P*<0.01 (vs. LPS+Vector group).

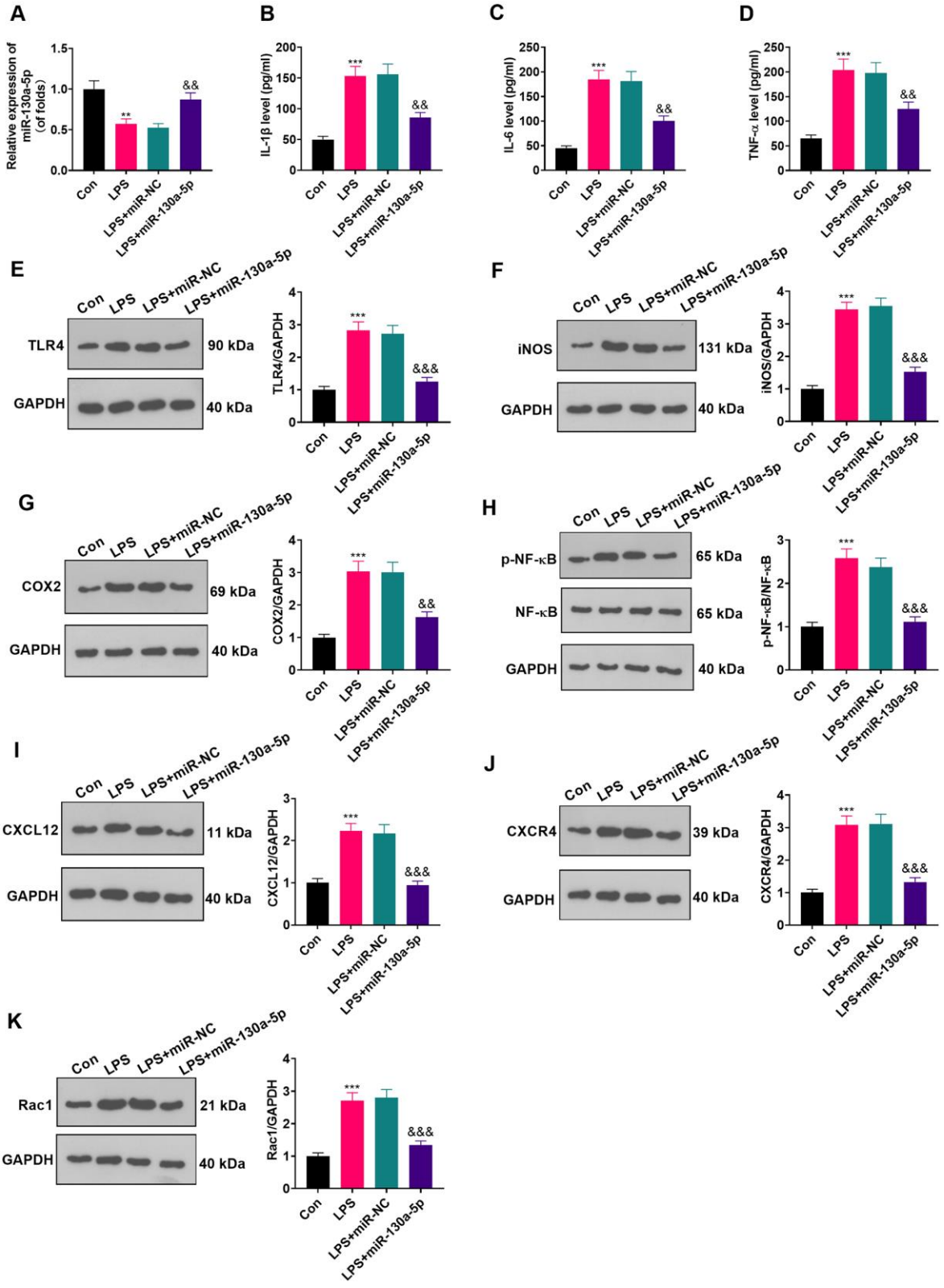

Figure 4. Up-regulating miR-130a-5p suppressed LPS-induced inflammation in astrocytes. (**A**) After transfection of miR-130a-5p mimics, the mRNA level of miR-130a-5p in astrocytes was tested by RT-qPCR. (**B**–**D**) The contents of IL-1β (**B**), IL-6 (**C**) and TNF-α (**D**) in astrocytes were compared by ELISA after up-regulation of miR-130a-5p. (**E**–**H**) WB detected the expression of TLR4 (**E**), iNOS (**F**), COX2(**G**), NF-κB (**H**), CXCL12 (**I**), CXCR4 (**J**), and Rac1 (**K**) in astrocytes after up-regulating miR-130a-5p. Data were expressed as mean±SD. n=3. ***P*<0.01, ****P*<0.001 (vs. LPS group). &*P*<0.05, &&*P*<0.01 (vs. LPS+miR-NC group).

COX2, and phosphorylated NF-κB, were substantially attenuated after transfection with miR-130a-5p mimics (Figure 6G; $P< 0.05$ vs. the LPS+MEG3 group). These results manifested that MEG3 aggravated inflammation of LPS-induced astrocytes by targeting the miR-130a-5p/CXCL12 axis.

DISCUSSION

NP originates from the pathological nervous system, clinically characterized by spontaneous pain (persistent, paroxysmal) and induced pain (hyperalgesia, abnormal pain) [29]. Reactive astrocyte-mediated neuro-inflammation in the spinal dorsal horn contributes to NP [30]. Several studies have confirmed that inactivating astrocytes alleviates NP [31, 32]. LPS has been widely applied to activate glia *in vitro* [33]. Therefore, we employed CCI and LPS to construct experimental models in rats and astrocytes, respectively. This study revealed that MEG3 was up-regulated in spinal cord tissues of CCI rats and LPS-induced astrocytes. Furthermore, MEG3 activated the CXCL12/CXCR4 pathway by sponging miR-130a-5p, so as to aggravate NP in CCI rats and induce astrocytes. Our study may provide a new therapeutic target for NP.

Emerging evidence reveals that lncRNAs contribute to NP [34]. For instance, lncRNA XIST [35], lncRNA LINC00657 [36], and lncRNA NEAT1 [37] are all up-regulated in the CCI-induced NP model. Down-regulating them significantly lightens NP by repressing inflammatory response through attenuation of COX-2, TNF-α and IL-6. Additionally, lncRNAs play a prominent role in mediating astrocyte activation. Inhibition both lncRNA SNHG5 [38] and lncRNA GM14461 [39] dampens NP progression by inactivating astrocytes. On the other hand, MEG3 is widely involved in neuroinflammation. For example, up-regulating MEG3 ameliorates cognitive impairment, attenuates neuronal damage and abates astrocyte activation in Alzheimer's disease (AD) rat hippocampal tissues by choking the PI3K/Akt pathway [40]. Besides, MEG3 is up-regulated in traumatic brain injury (TBI), and up-regulated MEG3 boosts microglial activation and exacerbates TBI [12]. Meanwhile, MEG3 is highly expressed in the MACO rat model. Inhibiting the

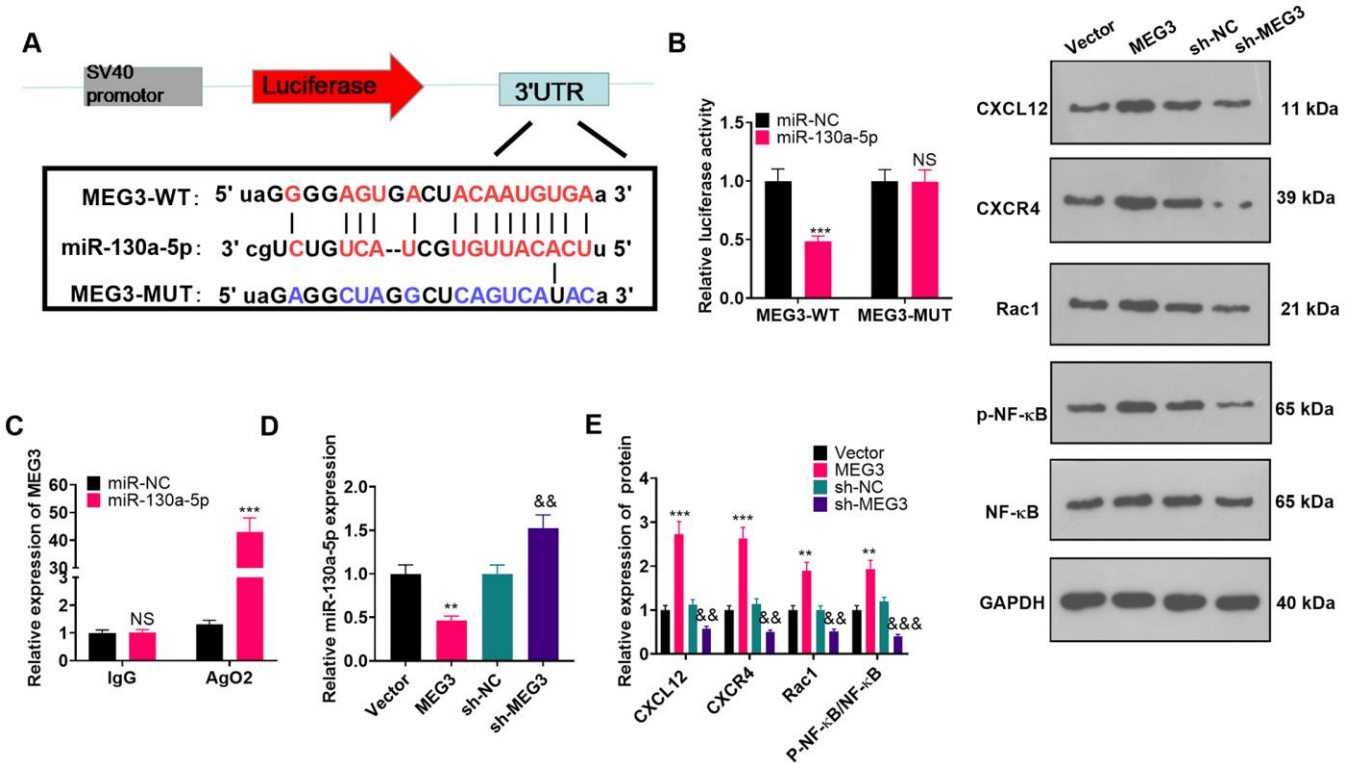

Figure 5. MEG3 targeted miR-130-a-5p. (**A**) Binding locations between MEG3 and miR-130a-5p were predicted using the starbase v2.0 database. (**B**) The target association between MEG3 and miR-130a-5p in astrocytes was clarified by the dual-luciferase reporter assay. (**C**) RIP was implemented to monitor the binding relationship between MEG3 and miR-130a-5p in astrocytes. NSP>0.05, ***P<0.001(vs. miR-NC group). (**D**) The miR-130a-5p expression in astrocytes after up-regulation or down-regulation of MEG3 was gauged by RT-qPCR. (**E**) WB was conducted to test the expression of CXCL12, CXCR4, Rac1 and NF-κB in astrocytes after up-regulating or down-regulating MEG3. Data were expressed as mean±SD. n=3. **P<0.01, ***P<0.001 (vs. Vector group). &P<0.05, &&P<0.01 (vs. sh-NC group).

MEG3 expression improves the nerve injury and reduces the cerebral infarction area, blood-brain barrier permeability and neuronal apoptosis of MCAO rats [41]. Those studies confirmed that MEG3 has remarkable significance in affecting neuroinflammation. Nevertheless, the specific role of MEG3 in NP of CCI model rats remains unclear. Here, we discovered that MEG3 was up-regulated in spinal cord tissues of CCI rats and LPS-treated astrocytes. Through intrathecal injection of LV-MEG3 lentivirus, we ascertained that up-regulating MEG3 in the CCI model aggravated NP and elevated the levels of IL-1β, TNF-α and IL-6 in rats.

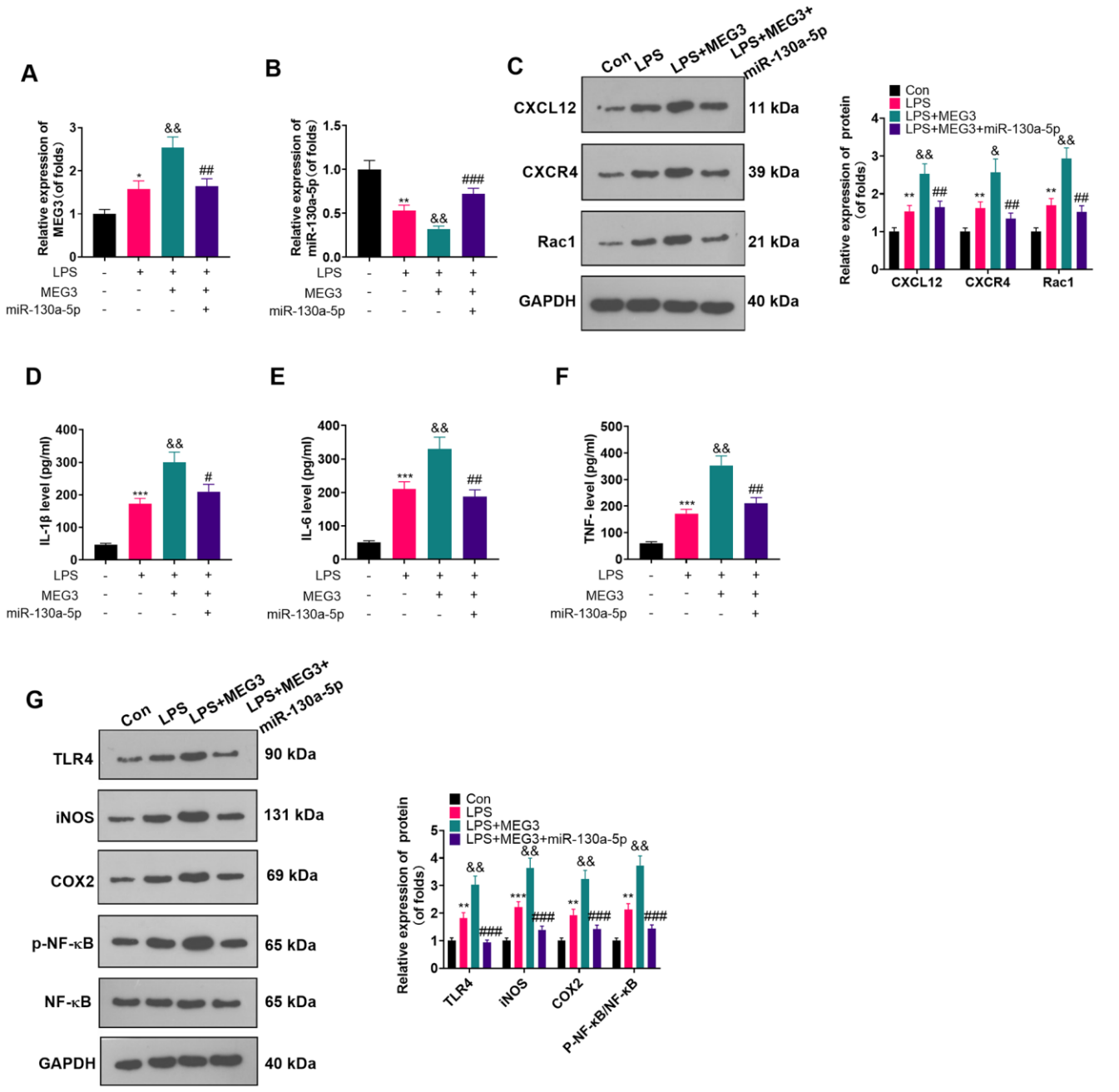

Figure 6. Overexpressing miR-130a-5p reversed the MEG3-mediated astrocyte inflammation. MEG3 overexpression plasmids and miR-130a-5p mimics were transfected in LPS-induced astrocytes. (**A**, **B**) The mRNA profiles of MEG3 and miR-130a-5p in astrocytes were tested by RT-qPCR. (**C**) The protein levels of CXCL12, CXCR4, and Rac1 in astrocytes were examined by WB. D-F: The concentrations of IL-1β (**D**), IL-6 (**E**) and TNF-α (**F**) in astrocytes were determined by ELISA. (**G**) WB was utilized to test the expression of TLR4, iNOS, COX2 and NF-κB in astrocytes. Data were expressed as mean±SD. n=3. **P*<0.05, ***P*<0.01, ****P*<0.001 (vs. Con group), #*P*<0.05, ##*P*<0.01 (vs. LPS group), &*P*<0.05, &&*P*<0.01, &&&*P*<0.001 (vs. LPS+MEG3 group).

Dysregulation of miR-130a-5p is associated with diversified inflammatory diseases [42–44]. Additionally, miR-130a-3p is signally overexpressed in rats with spinal cord injury (SCI)-induced NP and in LPS-induced BV2 microglia. Inhibiting miR-130a-3p expression activates IGF-1/IGF-1R, thereby abating SCI-induced NP [45]. Nevertheless, our study yielded different results, which were related to different downstream targets of miR-130a-5p. We found that miR-130a-5p expression decreased time-dependently in spinal cord tissues of CCI rats and LPS-induced astrocytes [25]. In parallel, miR-130a-5p mimics' transfection elevated miR-130a-5p expression, which suppressed LPS-induced inflammation in astrocytes.

CXCL12 is a specific chemokine ligand that contributes to cell chemotaxis. Upon binding to CXCR4, CXCL12 activates different signaling cascades to modulate cell proliferation, migration and metabolism [46]. The CXCL12/CXCR4 signal axis is involved in modulating NP [47]. Mai CL et al. found that CXCL12 gained an elevated level in circulating monocytes and plasma of patients with chronic pain. Blocking the CXCL12-CXCR4 signal transduction reduces the aggregation of peri-cerebrovascular macrophages in mouse hippocampus induced by nerve injury and alleviates neuroinflammation and resultant NP [48]. The expression of CXCL12 and CXCR4 in L4-5 spinal dorsal horn of SNI rats is up-regulated. Administration of CXCR4 antagonist AMD3100 declines the mechanical hypersensitivity induced by SNI rats [49], which has also been confirmed in previous studies [50, 51]. Here, CXCL12/CXCR4 is up-regulated in CCI rats, and overexpressing miR-130a-5p attenuates the MEG3-mediated inflammation in astrocytes by impeding CXCL12/CXCR4 expression.

The toll-like receptor 4 (TLR4)/nuclear factor-κB (NF-κB) axis is activated following CCI-induced NP [52]. It is often recognized as a vital pathway in charge of inflammatory cytokines expression and release [53]. Targeting the TLR4 pathway improves NP. For instance, intrathecal administration of LvOn-TLR4 small interfering (si)RNA (si-TLR4) prevents allodynia and hyperalgesia in CCI rats [54]. In another study, tizanidine, a highly selective α2-adrenoceptors (α2-AR) agonist, dampens spared nerve injury (SNI)-induced mechanical and thermal hyperalgesia by restraining the production of IL-1β, IL-6 and TNF-α, as well as the activation of TLR4/NF-κB [55]. Additionally, targeting CXCR4-mediated inflammation is associated with TLR4 signal inhibition [56, 57]. Our study indicated that MEG3 up-regulated the CXCL12/CXCR4/Rac1 axis and the TLR4/NF-κB pathway by abating miR-130a-5p. miR-130a-5p overexpression choked CXCL12/CXCR4/Rac1 and suppressed TLR4/NF-κB.

Overall, our study suggests that MEG3/miR-130a-5p/CXCL12/CXCR4 was altered in the CCI-induced NP rat model. Up-regulating MEG3 exacerbates NP and intensifies neuroinflammation. Moreover, MEG3 targets miR-130a-5p to elevate CXCL12/CXCR4 expression, which provides a potential prognostic marker and target for NP.

Abbreviation

NP: Neuropathic pain; CCI: chronic constriction injury; LPS: lipopolysaccharide; miR: microRNA; RT-qPCR: reverse transcription-quantitative PCR; WB: western blot; ELISA: enzyme-linked immunosorbent assay; IHC: immunohistochemistry; RIP: immunoprecipitation; IL-6: interleukin-6; lncRNAs: non-coding RNAs; SNL: spinal nerve ligation; MEG3: Maternal expression gene 3; MCAO: middle cerebral artery occlusion; OGD: oxygen-glucose deprivation; PWT: paw withdrawal threshold; PWL: paw withdraw latency; RT: room temperature; TUNEL: TdT-mediated dUTP nick end labeling; AI: apoptosis index; FBS: fetal bovine serum; ATCC: American Type Culture Collection; NHAs: Normal human astrocytes; qRT-PCR: quantitative polymerase chain reaction; ELISA: Enzyme-linked immunosorbent assay; TBI: traumatic brain injury; AD: Alzheimer's disease; SCI: spinal cord injury.

AUTHOR CONTRIBUTIONS

Conceived and designed the experiments: Cheng Xu; Performed the experiments: Jiacai Dong; Statistical analysis: Rui Xia, Zhonggui Zhang; Wrote the paper: Jiacai Dong. All authors read and approved the final manuscript.

CONFLICTS OF INTEREST

The authors declare that they have no conflicts of interest.

FUNDING

This research did not receive any specific grant from funding agencies in the public, commercial, or not- for-profit sectors.

REFERENCES

1. Gilron I, Baron R, Jensen T. Neuropathic pain: principles of diagnosis and treatment. Mayo Clin Proc. 2015; 90:532–45. https://doi.org/10.1016/j.mayocp.2015.01.018 PMID:25841257

2. Basić-Kes V, Zavoreo I, Bosnar-Puretić M, Ivanković M, Bitunjac M, Govori V, Demarin V. Neuropathic pain. Acta Clin Croat. 2009; 48:359–65. PMID:20055264

3. Cavalli E, Mammana S, Nicoletti F, Bramanti P, Mazzon E. The neuropathic pain: An overview of the current treatment and future therapeutic approaches. Int J Immunopathol Pharmacol. 2019; 33:2058738419838383. https://doi.org/10.1177/2058738419838383 PMID:30900486

4. Miller YI, Navia-Pelaez JM, Corr M, Yaksh TL. Lipid rafts in glial cells: role in neuroinflammation and pain processing. J Lipid Res. 2020; 61:655–66. https://doi.org/10.1194/jlr.TR119000468 PMID:31862695

5. Szok D, Tajti J, Nyári A, Vécsei L. Therapeutic Approaches for Peripheral and Central Neuropathic Pain. Behav Neurol. 2019; 2019:8685954. https://doi.org/10.1155/2019/8685954 PMID:31871494

6. Wu S, Bono J, Tao YX. Long noncoding RNA (lncRNA): a target in neuropathic pain. Expert Opin Ther Targets. 2019; 23:15–20. https://doi.org/10.1080/14728222.2019.1550075 PMID:30451044

7. Zhang JY, Lv DB, Su YN, Wang XL, Sheng WC, Yang G, Li LX, Gao X, Gao YZ, Li JT. LncRNA SNHG1 attenuates neuropathic pain following spinal cord injury by regulating CDK4 level. Eur Rev Med Pharmacol Sci. 2020; 24:12034–40. https://doi.org/10.26355/eurrev_202012_23992 PMID:33336721

8. Tian Y, Sun L, Qi T. Long noncoding RNA GAS5 ameliorates chronic constriction injury induced neuropathic pain in rats by modulation of the miR-452-5p/CELF2 axis. Can J Physiol Pharmacol. 2020; 98:870–77. https://doi.org/10.1139/cjpp-2020-0036 PMID:33264082

9. Li G, Jiang H, Zheng C, Zhu G, Xu Y, Sheng X, Wu B, Guo J, Zhu S, Zhan Y, Lin W, Ding R, Zhang C, et al. Long noncoding RNA MRAK009713 is a novel regulator of neuropathic pain in rats. Pain. 2017; 158:2042–52. https://doi.org/10.1097/j.pain.0000000000001013 PMID:28708759

10. Kong C, Du J, Bu H, Huang C, Xu F, Ren H. LncRNA KCNA2-AS regulates spinal astrocyte activation through STAT3 to affect postherpetic neuralgia. Mol Med. 2020; 26:113. https://doi.org/10.1186/s10020-020-00232-9 PMID:33225882

11. Wen J, Yang Y, Wu S, Wei G, Jia S, Hannaford S, Tao YX. Long noncoding RNA H19 in the injured dorsal root ganglion contributes to peripheral nerve injury-induced pain hypersensitivity. Transl Perioper Pain Med. 2020; 7:176–84. PMID:32099850

12. Meng J, Ding T, Chen Y, Long T, Xu Q, Lian W, Liu W. LncRNA-Meg3 promotes Nlrp3-mediated microglial inflammation by targeting miR-7a-5p. Int Immunopharmacol. 2021; 90:107141. https://doi.org/10.1016/j.intimp.2020.107141 PMID:33189612

13. Li G, Liu Y, Meng F, Xia Z, Wu X, Fang Y, Zhang C, Zhang Y, Liu D. LncRNA MEG3 inhibits rheumatoid arthritis through miR-141 and inactivation of AKT/mTOR signalling pathway. J Cell Mol Med. 2019; 23:7116–20. https://doi.org/10.1111/jcmm.14591 PMID:31411001

14. Li Y, Zhang S, Zhang C, Wang M. LncRNA MEG3 inhibits the inflammatory response of ankylosing spondylitis by targeting miR-146a. Mol Cell Biochem. 2020; 466:17–24. https://doi.org/10.1007/s11010-019-03681-x PMID:31894531

15. Li X, Tang C, Wang J, Guo P, Wang C, Wang Y, Zhang Z, Wu H. Methylene blue relieves the development of osteoarthritis by upregulating lncRNA MEG3. Exp Ther Med. 2018; 15:3856–64. https://doi.org/10.3892/etm.2018.5918 PMID:29581742

16. Li T, Luo Y, Zhang P, Guo S, Sun H, Yan D, Liu X, Yang B. LncRNA MEG3 regulates microglial polarization through KLF4 to affect cerebral ischemia-reperfusion injury. J Appl Physiol (1985). 2020; 129:1460–67. https://doi.org/10.1152/japplphysiol.00433.2020 PMID:33180644

17. Zhou XM, Liu J, Wang Y, Zhang MH. Silencing of long noncoding RNA MEG3 enhances cerebral protection of dexmedetomidine against hypoxic-ischemic brain damage in neonatal mice by binding to miR-129-5p. J Cell Biochem. 2018. [Epub ahead of print]. https://doi.org/10.1002/jcb.28075 PMID:30485519

18. Xie B, Qiao M, Xuan J. lncRNA MEG3 Downregulation Relieves Intracerebral Hemorrhage by Inhibiting Oxidative Stress and Inflammation in an miR-181b-Dependent Manner. Med Sci Monit. 2021; 27:e929435. https://doi.org/10.12659/MSM.929435 PMID:34267173

19. Zhou Y, Cao HB, Li WJ, Zhao L. The CXCL12 (SDF-1)/CXCR4 chemokine axis: Oncogenic properties, molecular targeting, and synthetic and natural product

CXCR4 inhibitors for cancer therapy. Chin J Nat Med. 2018; 16:801–10.
https://doi.org/10.1016/S1875-5364(18)30122-5
PMID:30502762

20. Liu ZY, Song ZW, Guo SW, He JS, Wang SY, Zhu JG, Yang HL, Liu JB. CXCL12/CXCR4 signaling contributes to neuropathic pain via central sensitization mechanisms in a rat spinal nerve ligation model. CNS Neurosci Ther. 2019; 25:922–36.
https://doi.org/10.1111/cns.13128
PMID:30955244

21. Huang W, Zheng W, Liu S, Zeng W, Levitt RC, Candiotti KA, Lubarsky DA, Hao S. HSV-mediated p55TNFSR reduces neuropathic pain induced by HIV gp120 in rats through CXCR4 activity. Gene Ther. 2014; 21:328–36.
https://doi.org/10.1038/gt.2013.90
PMID:24451118

22. Li R, Fang L, Pu Q, Bu H, Zhu P, Chen Z, Yu M, Li X, Weiland T, Bansal A, Ye SQ, Wei Y, Jiang J, Wu M. MEG3-4 is a miRNA decoy that regulates IL-1β abundance to initiate and then limit inflammation to prevent sepsis during lung infection. Sci Signal. 2018; 11:eaao2387.
https://doi.org/10.1126/scisignal.aao2387
PMID:29945883

23. Li Y, Zhang H, Li Z, Yan X, Li Y, Liu S. microRNA-130a-5p suppresses myocardial ischemia reperfusion injury by downregulating the HMGB2/NF-κB axis. BMC Cardiovasc Disord. 2021; 21:121.
https://doi.org/10.1186/s12872-020-01742-4
PMID:33658008

24. Sui S, Sun L, Zhang W, Li J, Han J, Zheng J, Xin H. LncRNA MEG8 Attenuates Cerebral Ischemia After Ischemic Stroke Through Targeting miR-130a-5p/VEGFA Signaling. Cell Mol Neurobiol. 2021; 41:1311–24.
https://doi.org/10.1007/s10571-020-00904-4
PMID:32627090

25. Dong J, Xu C, Xia R, Zhang Z. Upregulating miR-130a-5p relieves astrocyte over activation-induced neuropathic pain through targeting C-X-C motif chemokine receptor 12/C-X-C motif chemokine receptor 4 axis. Neuroreport. 2021; 32:135–43.
https://doi.org/10.1097/WNR.0000000000001573
PMID:33395188

26. Chu LW, Cheng KI, Chen JY, Cheng YC, Chang YC, Yeh JL, Hsu JH, Dai ZK, Wu BN. Loganin prevents chronic constriction injury-provoked neuropathic pain by reducing TNF-α/IL-1β-mediated NF-κB activation and Schwann cell demyelination. Phytomedicine. 2020; 67:153166.
https://doi.org/10.1016/j.phymed.2019.153166
PMID:31955133

27. Wu J, Wang C, Ding H. LncRNA MALAT1 promotes neuropathic pain progression through the miR-154-5p/AQP9 axis in CCI rat models. Mol Med Rep. 2020; 21:291–303.
https://doi.org/10.3892/mmr.2019.10829
PMID:31746418

28. Pan X, Shen C, Huang Y, Wang L, Xia Z. Loss of SNHG4 Attenuated Spinal Nerve Ligation-Triggered Neuropathic Pain through Sponging miR-423-5p. Mediators Inflamm. 2020; 2020:2094948.
https://doi.org/10.1155/2020/2094948
PMID:32454787

29. Baron R. Neuropathic pain: a clinical perspective. Handb Exp Pharmacol. 2009; 129:3–30.
https://doi.org/10.1007/978-3-540-79090-7_1
PMID:19655103

30. Nong X, Lan Y. Picroside II Attenuates CCI-Induced Neuropathic Pain in Rats by Inhibiting Spinal Reactive Astrocyte-Mediated Neuroinflammation Through the NF-κB Pathway. Neurochem Res. 2018; 43:1058–66.
https://doi.org/10.1007/s11064-018-2518-7
PMID:29671236

31. Lee JY, Choi HY, Ju BG, Yune TY. Estrogen alleviates neuropathic pain induced after spinal cord injury by inhibiting microglia and astrocyte activation. Biochim Biophys Acta Mol Basis Dis. 2018; 1864:2472–80.
https://doi.org/10.1016/j.bbadis.2018.04.006
PMID:29653184

32. Li R, Dang S, Yao M, Zhao C, Zhang W, Cui J, Wang J, Wen A. Osthole alleviates neuropathic pain in mice by inhibiting the $P2Y_1$-receptor-dependent JNK signaling pathway. Aging (Albany NY). 2020; 12:7945–62.
https://doi.org/10.18632/aging.103114
PMID:32365053

33. Solà C, Casal C, Tusell JM, Serratosa J. Astrocytes enhance lipopolysaccharide-induced nitric oxide production by microglial cells. Eur J Neurosci. 2002; 16:1275–83.
https://doi.org/10.1046/j.1460-9568.2002.02199.x
PMID:12405988

34. Li Z, Li X, Chen X, Li S, Ho IH, Liu X, Chan MT, Wu WK. Emerging roles of long non-coding RNAs in neuropathic pain. Cell Prolif. 2019; 52:e12528.
https://doi.org/10.1111/cpr.12528 PMID:30362191

35. Yan XT, Lu JM, Wang Y, Cheng XL, He XH, Zheng WZ, Chen H, Wang YL. XIST accelerates neuropathic pain progression through regulation of miR-150 and ZEB1 in CCI rat models. J Cell Physiol. 2018; 233:6098–106.
https://doi.org/10.1002/jcp.26453 PMID:29323698

36. Shen F, Zheng H, Zhou L, Li W, Zhang Y, Xu X. LINC00657 expedites neuropathic pain development by modulating miR-136/ZEB1 axis in a rat model. J Cell

Biochem. 2019; 120:1000–10.
https://doi.org/10.1002/jcb.27466
PMID:30203524

37. Xia LX, Ke C, Lu JM. NEAT1 contributes to neuropathic pain development through targeting miR-381/HMGB1 axis in CCI rat models. J Cell Physiol. 2018; 233:7103–11.
https://doi.org/10.1002/jcp.26526 PMID:29633273

38. Chen M, Yang Y, Zhang W, Li X, Wu J, Zou X, Zeng X. Long Noncoding RNA SNHG5 Knockdown Alleviates Neuropathic Pain by Targeting the miR-154-5p/CXCL13 Axis. Neurochem Res. 2020; 45:1566–75.
https://doi.org/10.1007/s11064-020-03021-2
PMID:32248399

39. Cai J, Yan Y, Zhang D, Zhu M, Wang Z, Zhang X, Xu M. Silencing of lncRNA Gm14461 alleviates pain in trigeminal neuralgia through inhibiting astrocyte activation. IUBMB Life. 2020; 72:2663–71.
https://doi.org/10.1002/iub.2395 PMID:33141516

40. Yi J, Chen B, Yao X, Lei Y, Ou F, Huang F. Upregulation of the lncRNA MEG3 improves cognitive impairment, alleviates neuronal damage, and inhibits activation of astrocytes in hippocampus tissues in Alzheimer's disease through inactivating the PI3K/Akt signaling pathway. J Cell Biochem. 2019; 120:18053–65.
https://doi.org/10.1002/jcb.29108
PMID:31190362

41. You D, You H. Repression of long non-coding RNA MEG3 restores nerve growth and alleviates neurological impairment after cerebral ischemia-reperfusion injury in a rat model. Biomed Pharmacother. 2019; 111:1447–57.
https://doi.org/10.1016/j.biopha.2018.12.067
PMID:30841460

42. Choi EJ, Kim HB, Baek YH, Kim EH, Pascua PN, Park SJ, Kwon HI, Lim GJ, Kim S, Kim YI, Choi YK. Differential microRNA expression following infection with a mouse-adapted, highly virulent avian H5N2 virus. BMC Microbiol. 2014; 14:252.
https://doi.org/10.1186/s12866-014-0252-0
PMID:25266911

43. Zhang M, Zhao S, Xu C, Shen Y, Huang J, Shen S, Li Y, Chen X. Ablation of lncRNA MIAT mitigates high glucose-stimulated inflammation and apoptosis of podocyte via miR-130a-3p/TLR4 signaling axis. Biochem Biophys Res Commun. 2020; 533:429–36.
https://doi.org/10.1016/j.bbrc.2020.09.034
PMID:32972755

44. Su S, Zhao Q, He C, Huang D, Liu J, Chen F, Chen J, Liao JY, Cui X, Zeng Y, Yao H, Su F, Liu Q, et al. miR-142-5p and miR-130a-3p are regulated by IL-4 and IL-13 and control profibrogenic macrophage program. Nat Commun. 2015; 6:8523.
https://doi.org/10.1038/ncomms9523 PMID:26436920

45. Yao L, Guo Y, Wang L, Li G, Qian X, Zhang J, Liu H, Liu G. Knockdown of miR-130a-3p alleviates spinal cord injury induced neuropathic pain by activating IGF-1/IGF-1R pathway. J Neuroimmunol. 2021; 351:577458.
https://doi.org/10.1016/j.jneuroim.2020.577458
PMID:33360969

46. Gao JH, Yu XH, Tang CK. CXC chemokine ligand 12 (CXCL12) in atherosclerosis: An underlying therapeutic target. Clin Chim Acta. 2019; 495:538–44.
https://doi.org/10.1016/j.cca.2019.05.022
PMID:31145896

47. Zou Y, Cao Y, Liu Y, Zhang X, Li J, Xiong Y. The role of dorsal root ganglia PIM1 in peripheral nerve injury-induced neuropathic pain. Neurosci Lett. 2019; 709:134375.
https://doi.org/10.1016/j.neulet.2019.134375
PMID:31349016

48. Mai CL, Tan Z, Xu YN, Zhang JJ, Huang ZH, Wang D, Zhang H, Gui WS, Zhang J, Lin ZJ, Meng YT, Wei X, Jie YT, et al. CXCL12-mediated monocyte transmigration into brain perivascular space leads to neuroinflammation and memory deficit in neuropathic pain. Theranostics. 2021; 11:1059–78.
https://doi.org/10.7150/thno.44364 PMID:33391521

49. Bai L, Wang X, Li Z, Kong C, Zhao Y, Qian JL, Kan Q, Zhang W, Xu JT. Upregulation of Chemokine CXCL12 in the Dorsal Root Ganglia and Spinal Cord Contributes to the Development and Maintenance of Neuropathic Pain Following Spared Nerve Injury in Rats. Neurosci Bull. 2016; 32:27–40.
https://doi.org/10.1007/s12264-015-0007-4
PMID:26781879

50. Yu Y, Huang X, Di Y, Qu L, Fan N. Effect of CXCL12/CXCR4 signaling on neuropathic pain after chronic compression of dorsal root ganglion. Sci Rep. 2017; 7:5707.
https://doi.org/10.1038/s41598-017-05954-1
PMID:28720830

51. Xing F, Kong C, Bai L, Qian J, Yuan J, Li Z, Zhang W, Xu JT. CXCL12/CXCR4 signaling mediated ERK1/2 activation in spinal cord contributes to the pathogenesis of postsurgical pain in rats. Mol Pain. 2017; 13:1744806917718753.
https://doi.org/10.1177/1744806917718753
PMID:28633557

52. Iannotta M, Belardo C, Trotta MC, Iannotti FA, Vitale RM, Maisto R, Boccella S, Infantino R, Ricciardi F, Mirto BF, Ferraraccio F, Panarese I, Amodeo P, et al. N-palmitoyl-D-glucosamine, a Natural Monosaccharide-Based Glycolipid, Inhibits TLR4 and Prevents LPS-

Induced Inflammation and Neuropathic Pain in Mice. Int J Mol Sci. 2021; 22:1491. https://doi.org/10.3390/ijms22031491 PMID:33540826

53. Rahimifard M, Maqbool F, Moeini-Nodeh S, Niaz K, Abdollahi M, Braidy N, Nabavi SM, Nabavi SF. Targeting the TLR4 signaling pathway by polyphenols: A novel therapeutic strategy for neuroinflammation. Ageing Res Rev. 2017; 36:11–19. https://doi.org/10.1016/j.arr.2017.02.004 PMID:28235660

54. Liu Y, Zhang Y, Pan R, Chen M, Wang X, Kong E, Yu W, Sun Y, Wu F. Lentiviral-mediated inducible silencing of TLR4 attenuates neuropathic pain in a rat model of chronic constriction injury. Mol Med Rep. 2018; 18:5545–51. https://doi.org/10.3892/mmr.2018.9560 PMID:30365084

55. Pei W, Zou Y, Wang W, Wei L, Zhao Y, Li L. Tizanidine exerts anti-nociceptive effects in spared nerve injury model of neuropathic pain through inhibition of TLR4/NF-κB pathway. Int J Mol Med. 2018; 42:3209–19. https://doi.org/10.3892/ijmm.2018.3878 PMID:30221670

56. Yu SJ, Wu KJ, Wang YS, Song JS, Wu CH, Jan JJ, Bae E, Chen H, Shia KS, Wang Y. Protective Effect of CXCR4 Antagonist CX807 in a Rat Model of Hemorrhagic Stroke. Int J Mol Sci. 2020; 21:7085. https://doi.org/10.3390/ijms21197085 PMID:32992950

57. Li XQ, Zhang ZL, Tan WF, Sun XJ, Ma H. Down-Regulation of CXCL12/CXCR4 Expression Alleviates Ischemia-Reperfusion-Induced Inflammatory Pain via Inhibiting Glial TLR4 Activation in the Spinal Cord. PLoS One. 2016; 11:e0163807. https://doi.org/10.1371/journal.pone.0163807 PMID:27760212